Journal of Innate Immunity

Research Article

J Innate Immun 2023;15:865–875
DOI: 10.1159/000534736

Received: May 5, 2023
Accepted: October 18, 2023
Published online: November 18, 2023

Human Ribonuclease 6 Has a Protective Role during Experimental Urinary Tract Infection

Juan de Dios Ruiz-Rosado[a, b] Hanna Cortado[a] Macie Kercsmar[a] Birong Li[a] Gregory Ballash[a] Israel Cotzomi-Ortega[a] Yuriko I. Sanchez-Zamora[a] Sudipti Gupta[a] Christina Ching[a, c] Ester Boix[d] Ashley R. Jackson[a, b] John David Spencer[a, b] Brian Becknell[a, b]

[a]Kidney and Urinary Tract Center, The Abigail Wexner Research Institute at Nationwide Children's, Columbus, OH, USA; [b]Division of Nephrology and Hypertension, Nationwide Children's Hospital, Columbus, OH, USA; [c]Department of Urology, Nationwide Children's Hospital, Columbus, OH, USA; [d]Department of Biochemistry and Molecular Biology, Faculty of Biosciences, Universitat Autònoma De Barcelona, Barcelona, Spain

Keywords
Antimicrobial peptides · Bacterial infection · Macrophage · Host defense · Urinary tract infection · Cystitis

Abstract
Mounting evidence suggests that antimicrobial peptides and proteins (AMPs) belonging to the RNase A superfamily have a critical role in defending the bladder and kidney from bacterial infection. RNase 6 has been identified as a potent, leukocyte-derived AMP, but its impact on urinary tract infection (UTI) in vivo has not been demonstrated. To test the functional role of human RNase 6, we generated *RNASE6* transgenic mice and studied their susceptibility to experimental UTI. In addition, we generated bone marrow-derived macrophages to study the impact of RNase 6 on antimicrobial activity within a cellular context. When subjected to experimental UTI, *RNASE6* transgenic mice developed reduced uropathogenic *Escherichia coli* (UPEC) burden, mucosal injury, and inflammation compared to non-transgenic controls. Monocytes and macrophages were the predominant cellular sources of RNase 6 during UTI, and *RNASE6* transgenic macrophages were more proficient at intracellular UPEC killing than non-transgenic controls. Altogether, our findings indicate a protective role for human RNase 6 during experimental UTI.

Introduction

Urinary tract infections (UTIs) rank among the most common bacterial infections of childhood [1]. UTIs occur in 2% of males and 8% of females prior to 7 years of age, and 12–30% of these children will develop recurrent UTI [2–4]. Young children with UTI have a 50% risk of pyelonephritis, which is associated with acute kidney injury and new renal scars in 15% of cases. Antibiotic options to treat UTIs are limited by rising bacterial

Juan de Dios Ruiz-Rosado and Hanna Cortado contributed equally to this work.

karger@karger.com
www.karger.com/jin

Correspondence to:
Brian Becknell, brian.becknell2@nationwidechildrens.org

resistance rates [5]. Novel, effective measures are desperately needed to identify patients most at risk for UTI recurrence, as well as to prevent detrimental sequelae like urosepsis, acute kidney injury, and renal scarring.

To destroy invading uropathogens, the innate immune system relies on a combination of phagocyte recruitment, complement activation, and production of antimicrobial peptides and proteins (AMPs) [6–8]. AMPs confer antimicrobial activity by disrupting membranes, inducing microbial agglutination, blocking cell division, and impairing prokaryotic translational machinery, among others [9–11]. AMPs have been implicated in host defense against UTI, based on their potent antimicrobial activity toward uropathogenic bacteria in vitro, as well as their potential to attenuate host susceptibility to experimental UTI in vivo. Multiple cell types produce AMPs during UTI, including urothelial cells, kidney intercalated cells, neutrophils, monocytes, and macrophages [7, 12–14].

Macrophages have been implicated as effectors of the innate immune response during UTI [15–20]. Depletion of circulating monocytes with clodronate liposomes leads to impaired clearance of uropathogenic *Escherichia coli* (UPEC) during experimental cystitis [16, 17]. In the infected bladder and kidney, resident Cx3cr1+ macrophages produce chemokines, which are instrumental in the recruitment of Ccr2+ monocytes and neutrophils to the site of infection [15, 17]. During cystitis, interactions between resident macrophages and recruited monocytes serve an instrumental role in promoting transepithelial migration of neutrophils to the urinary space [17]. However, the antimicrobial mechanisms by which macrophages confer resistance to UTI are incompletely understood. In particular, the antimicrobial roles of specific macrophage-derived AMPs have not yet been fully elucidated.

We previously identified RNase 6 as a monocyte and macrophage-derived AMP that is expressed in the urinary tracts of humans and mice [11]. Moreover, RNase 6 levels increase during experimental UTI in mice and in kidneys from human patients with chronic pyelonephritis [11]. Recombinant human and mouse RNase 6 proteins exhibited bactericidal activity toward UPEC at low-micromolar concentrations, along with absent cytotoxicity toward human epithelial cells and erythrocytes [11]. Despite these findings, the functional role of human RNase 6 during UTI in vivo remains to be elucidated. In this study, we generated mice bearing a human *RNASE6* transgene and investigated its impact on UTI susceptibility in vivo.

Materials and Methods

Study Approval. Animal experiments were approved by and performed in accordance with the National Institutes of Health Guide for the Care and Use of Laboratory Animals and the Institutional Animal Care and Use Committee at Abigail Wexner Research Institute at Nationwide Children's Hospital.

Generation of Human RNASE6 Transgenic Mice. Transgenic mice were generated by TransViragen (Research Triangle Park, NC, USA). BAC clone CH17-158G19 was digested in vitro with Cas9 and guide RNAs *RNASE6*-5g70T (protospacer sequence 5′-gTGTGATTGATGCTGTGCAA-3′) and *RNASE6*-3g68B (protospacer sequence 5′-gTGCAGGGTGAACTGACAGA) to remove a 30,054 bp fragment. The fragment was cloned into a BAC vector backbone to generate the pBAC-*RNASE6* Tg BAC. The Tg BAC was digested with PmeI and a 30,062 bp fragment was gel purified by standard methods (QIAquick Gel Extraction Kit). The isolated fragment was dialyzed in microinjection buffer and microinjected into C57BL/6J mouse embryos. Resulting animals were screened for the presence of the transgene by PCR using the following primers: sense 5′- CTCAGATGAGGCAGGAAGCA-3′ and antisense 5′-TTTACTGCTCTACTCGCTCCAG-3,′ yielding a 393 bp product. Founders were crossed with C57BL/6J to generate *RNASE6* transgenic lines. In all experiments, *RNASE6* mice transgenic were compared to age- and sex-matched littermate controls that lacked the *RNASE6* transgene.

Characterization of Transgenic Mice. The Ohio State University Comparative Pathology and Mouse Phenotyping Shared Resource was used to measure serum chemistries (Alfa Wassermann VetACE Chemistry Analyzer; Diamond Diagnostics, Holliston, MA, USA), complete blood counts (Hemavet 950FS Hematology Analyzer; Drew Scientific, Miami Lakes, FL, USA), and evaluate baseline organ histology in healthy adult female *RNASE6* transgenic mice and non-transgenic littermates.

Experimental UTI. Experimental UTI was induced in anesthetized female mice age six to eight weeks by transurethral inoculation with UTI89, a clinical UPEC isolate from a patient with cystitis [21]. UTI89 was inoculated from a glycerol stock and grown statically in LB medium for 16 h at 37°C. The inoculum was 10^7 colony forming units (CFUs) in 50 μL phosphate buffered saline (PBS). After infection, mice were re-anesthetized and euthanized by exsanguination, urinary tract organs were isolated, and bacterial burden assessed [22]. Briefly, urinary tract tissues were homogenized by mechanical agitation with stainless steel beads (McMaster-Carr, Elmhurst, IL, USA) in sterile PBS using a TissueLyser II instrument (Qiagen, Germantown, MD, USA), serially diluted, and plated on LB agar for CFU enumeration. Alternatively, bladders were fixed in 10% formalin, embedded in paraffin, H&E stained, and mucosal injury and inflammation were scored by a veterinary pathologist in a blinded fashion [23, 24]. Intracellular bacterial communities were identified by β-galactosidase staining [25, 26].

qRT-PCR, Western blotting, and ELISA. Total RNA was isolated from indicated tissues using TRIzol Reagent (Thermo Fisher Scientific, Waltham, MA, USA), reverse transcribed into cDNA (Verso cDNA Synthesis Kit; Thermo Fisher Scientific), and subject to PCR using intron-spanning, gene-specific primers. Amplification was detected using SybrGreen (Absolute Blue qPCR SYBRGreen; Thermo Fisher) with an Applied Biosystems 7000 Real-Time PCR System (Thermo Fisher). Results were expressed

using the 2^{-ddCT} method normalizing to the housekeeping gene, *Gapdh*. The following gene-specific were used: human *RNASE6* forward 5′-AGCCCCAACACTGAGACCAGAAAA-3′ and reverse 5′-GGTGGCAGTTGTGCCGACGA-3′; mouse *Rnase6* forward 5′- TGGCCCTGTTCACCATAGGAGCC-3′ and reverse 5′-GCGCATGGCTGTGTTGCATGG-3′; and *Gapdh* forward 5′-CTGGAGAAACCTGCCAAGTA-3′ and reverse 5′-TGTTGC TGTAGCCGTATTCA-3.′ Protein extraction and Western blotting were performed as described [27]. Primary antibodies were rabbit α-Gapdh (Cell Signaling, Beverly, MA, USA) and rabbit α-human RNase 6 (Cloud-Clone Corp., Katy, TX, USA). RNase 6 levels in macrophage supernatants were measured by ELISA (Cloud-Clone).

Immunofluorescence Microscopy. Formalin-fixed, paraffin-embedded kidneys were sectioned at 4 μm. Following citrate-based antigen retrieval, immunolocalization was performed using the following primary antibodies: rabbit α-human RNase 6 (1:800; Cloud-Clone), chicken α-GFP (1:300, Abcam, Waltham, MA, USA), goat α-RFP (1:500, Rockland Immunochemicals, Limerick, PA, USA), and goat α-*E. coli* (1:800, Abcam). Cy3-and AlexaFluor 488-conjugated secondary antibodies raised in donkey were used (1:300; Jackson ImmunoResearch Laboratories, West Grove, PA, USA), coverslipped using Vectashield with DAPI (Vector Laboratories, Burlingame, CA, USA), and imaged at ×60 using a Nikon Eclipse Ti2 microscope. Non-transgenic tissues were processed in parallel to confirm that findings were transgene specific. Additional negative control sections were incubated with irrelevant species-specific Ab or secondary Ab alone.

Flow Cytometry. Bladders were minced and digested in HBSS with 1 mg/mL collagenase type 4, 20 mg/mL DNase I, and 1 mg/mL BSA/fraction V (Invitrogen, Grand Island, NY, USA). After enzymatic dissociation, mononuclear and polymorphonuclear cells were enriched using a double gradient formed by layering an equal volume of Histopaque-1077 (Sigma, St. Louis, MO, USA) over Histopaque-1119 (Sigma). Single-cell suspensions were incubated in 1 mg/mL of anti-mouse Fc receptor (anti-mouse anti-CD16/32, clone 93) in 100 mL PBS containing 0.5% BSA plus 0.02% sodium (Na) azide (FACS buffer) for 15 min on ice to block nonspecific Ab binding. Cells were then stained with blue-fluorescent reactive dye (L23105; Life Technologies) for 20 min at room temperature to remove dead cells from the analysis. After washing, 1–3 million cells were stained for cell-surface receptors in FACS buffer, for 15 min at 4°C, with various fluorescent mAb combinations (see the list below). Flow cytometry studies used Abs at 1:100 dilutions. Stained cells were further collected on a LSR II cytofluorometer (BD Biosciences), and data were analyzed using FlowJo software (Tree Star, Ashland, OR, USA). Absolute cell numbers were calculated using CountBright Absolute Counting Beads (Thermo Fisher, Wilmington, DE, USA). The following fluorochrome-conjugated Abs were purchased from BioLegend: Brilliant Violet 650 anti-mouse I-A/I-E Ab (107641, M5/114.15.2), APC anti-mouse F4/80 Ab (123116, BM8), Brilliant Violet 785 anti-mouse CD45 Ab (103149, 30-F11), AlexaFluor 700 anti-mouse/human CD11b Ab (101222, M1/70), PerCP/Cy5.5 anti-mouse Ly-6G Ab (127616, 1A8), PE anti-mouse Ly-6C Ab (clone 128018, HK1.4).

UPEC Killing by Bone Marrow-Derived Macrophages. Mouse bone marrow-derived macrophages (BMDM) were derived by plating cells from femurs and tibia in DMEM F12 medium supplemented with 10% fetal bovine serum, 100 U/ml penicillin, 100 μg/mL streptomycin, 2 mM L-glutamine, and 20 ng/mL M-CSF (Biolegend, San Diego, CA, USA). After 6 days of culture at 37°C in 5% CO_2, cells were detached and plated into 24-well plates in the absence of antibiotics at 200,000 cells/well. The following day, UPEC-containing medium was added at the indicated multiplicity of infection (MOI) and centrifuged 750 *g* for 5 min to promote attachment. Extracellular and attached UPEC were enumerated as described after 30 min culture at 37°C [28]. Alternatively, after three washes with medium containing 100 μg/mL gentamicin, BMDM were incubated for an additional 120 min at 37°C followed by BMDM lysis with 0.1% Triton X-100 to enumerate intracellular UPEC [29]. Six replicate wells were evaluated for each experimental condition.

Cytokine Elicitation. BMDM from WT and *RNASE6* transgenic mice were cultured in DMEM F12 medium supplemented with 10% fetal bovine serum and challenged with UPEC (MOI 10) for 24 h. The supernatants were collected and stored at −80°C. The LEGENDplex Mouse Inflammation Panel Assay (Biolegend) was performed according to the manufacturer's directions to quantitate IL-1 α, TNF-α, MCP-1, IL-1β, IL-6, IL-10, IL-27, and IFN-β levels in supernatants. The samples were acquired with an LSR II flow cytometer (BD) and analyzed using the LEGENDplex™ Data Analysis Software Suite.

Macrophage Apoptosis and Necrosis. WT and *RNASE6* transgenic BMDMs were stimulated with UPEC (MOI 10) for 30 min and 3 h to evaluate early apoptosis and late apoptosis/necrosis, respectively. Cells undergoing apoptosis and/or necrosis were identified by the Pacific Blue Annexin V Apoptosis Detection Kit with 7-AAD (Biolegend). BMDMs were acquired by flow cytometry and analyzed with the FlowJo software.

Macrophage Phagocytosis. 2×10^5 BMDM from WT and *RNASE6* transgenic mice were cultured in RPMI-1640 medium (Sigma, R7509) supplemented with 10% fetal bovine serum using a black, clear bottom 96 well plate. After 30 min of culture at 37°C in 5% CO2, BMDMs were stimulated with Fluorescein-labeled *E. coli* K-12 Bioparticles (VybrantTM Phagocytosis Assay Kit, Invitrogen, V6694) following the manufacturer's protocol. After 15, 30, and 60 min, the cells were fixed using 4% PFA. The cells were washed twice with PBS, stained with trypan blue, 0.25 mg/mL, and imaged at 20X using an EVOS® FL Cell Imaging System microscope. Four areas were analyzed per well to assess the percentage of green (bioparticle) positive cells.

Statistics. Statistical analyses were performed using Prism Software (GraphPad Software, La Jolla, CA, USA). Continuous data were evaluated for a normal distribution with the D'Agostino-Pearson Omnibus test, with normality defined as a p value >0.05. Normally distributed data were compared by unpaired or paired t-test as appropriate; otherwise, the nonparametric Mann-Whitney U test was used with unpaired data. Multiple comparisons were made by one-way ANOVA with Tukey's modification with p values of <0.05 were considered significant.

Results

Establishment of Human RNASE6 Transgenic Mice. To investigate the functional role of RNase 6 in promoting bacterial clearance from the urinary tract in vivo, we developed human *RNASE6* transgenic mice (Fig. 1a). The

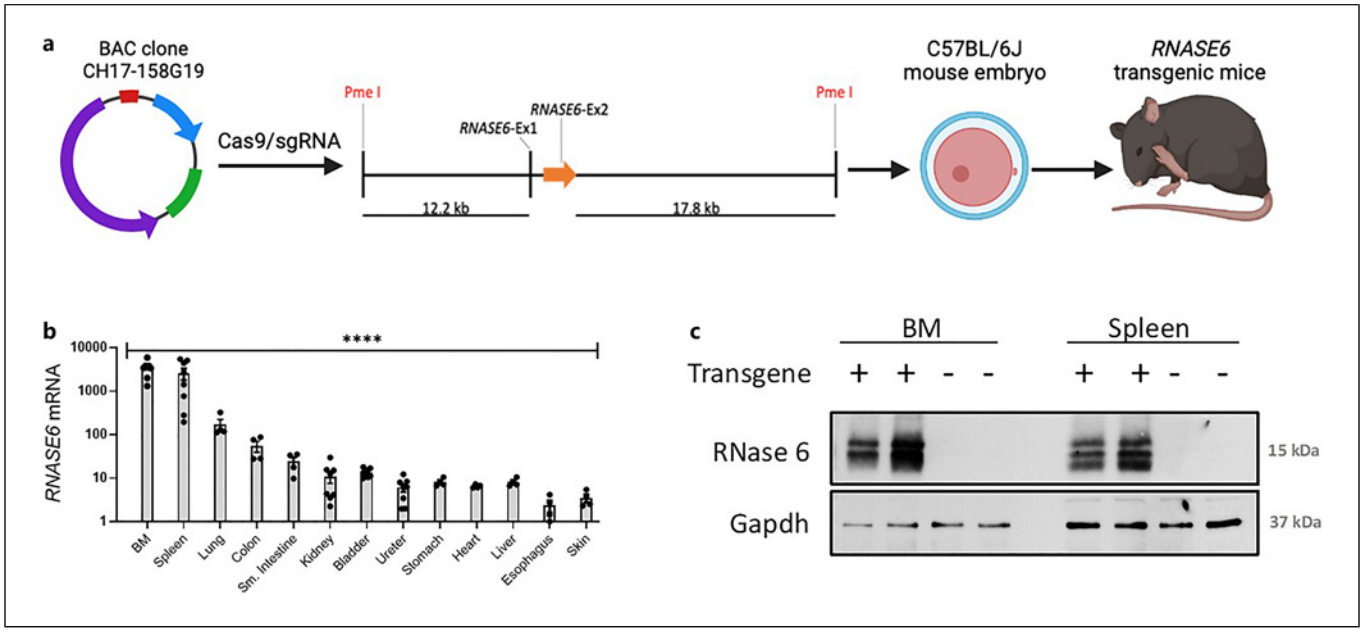

Fig. 1. Characterization of *RNASE6* transgenic mice. **a** Schematic of the BAC transgene containing human *RNASE6*. DNA lengths flanking *RNASE6* exons 1 (Ex1) and exons (Ex2) are shown in kilobases (kb). **b** Relative quantitation of *RNASE6* mRNA expression in transgenic tissues by QRT-PCR (n = 4–8 mice/group). ****$p <$ 0.0001, one-way ANOVA. Bars represent mean ± SEM for each condition. **c** Detection of RNase 6 protein expression in transgenic bone marrow (BM) and spleen by Western blotting.

30-kilobase transgene encompasses the *RNASE6* gene along with its putative regulatory elements and excludes any neighboring genes whose co-expression might confound the phenotype of transgenic mice. Two founders were generated and crossed with C57BL/6J mice to generate hemizygous *RNASE6* transgenic lines (online suppl. Fig. S1A; for all online suppl. material, see https://doi.org/10.1159/000534736). We selected one line (*RNASE6.22*) for further characterization based on higher magnitude of *RNASE6* mRNA and RNase 6 protein expression in F2 offspring (online suppl. Fig. S1B-C). Data from the *RNASE6.22* line are presented here.

We detected higher expression levels of *RNASE6* mRNA in hematopoietic organs, bone marrow and spleen, which are the primary sites of RNase 6 expression reported in humans and mice [11], with lower but detectable levels in the urinary tract (Fig. 1b). Western blotting with a polyclonal Ab directed against human RNase 6 identified 2–3 distinct bands in the range of 15-kilodalton (kDa) in bone marrow and spleen from transgenic mice that were absent in non-transgenic controls (Fig. 1c). The *RNASE6* transgene had no discernible impact on organ histology, body weight, complete blood count and differential, or serum chemistries (online suppl. Table S1). Flow cytometry determined that the number of neutrophils ($CD45^+/CD11B^+/Ly6C^-/Ly6G^+$), monocytes ($CD45^+/CD11B^+/Ly6G^-/Ly6C^+$), and macrophages ($Ly6C^-/Ly6G^-/MHC\text{-}II^+/F480^+$) in the bone marrow and spleen was comparable in *RNASE6* transgenic and WT mice (online suppl. Fig. S1D; gating strategies are shown in online suppl. Fig. S1E). These data demonstrate that the *RNASE6* transgene does not impact myelopoiesis and that *RNASE6* transgenic mice are healthy compared to their WT counterparts. Thus, *RNASE6* transgenic mice are well-suited for functional studies investigating the role of human RNase 6 in vivo.

Human RNase 6 Has a Protective Role during Experimental Cystitis. To investigate the role of human RNase 6 during UTI, we subjected female *RNASE6* transgenic mice to experimental cystitis. Following transurethral inoculation of UPEC strain UTI89, bladder RNase 6 protein levels increased within 6 h postinfection (hpi) and peaked 24 hpi (Fig. 2a). In contrast, there was no increase in *RNASE6* mRNA levels under these conditions, and *RNASE6* followed the same expression pattern as mouse *Rnase6* (online suppl. Fig. S2A). Splenic RNase 6 protein levels did not change 24 hpi, arguing against a systemic induction of RNase 6 (online suppl. Fig. S2B). When we measured bacterial burden 24 hpi, significantly fewer UPEC CFUs were recovered from the urine, bladder,

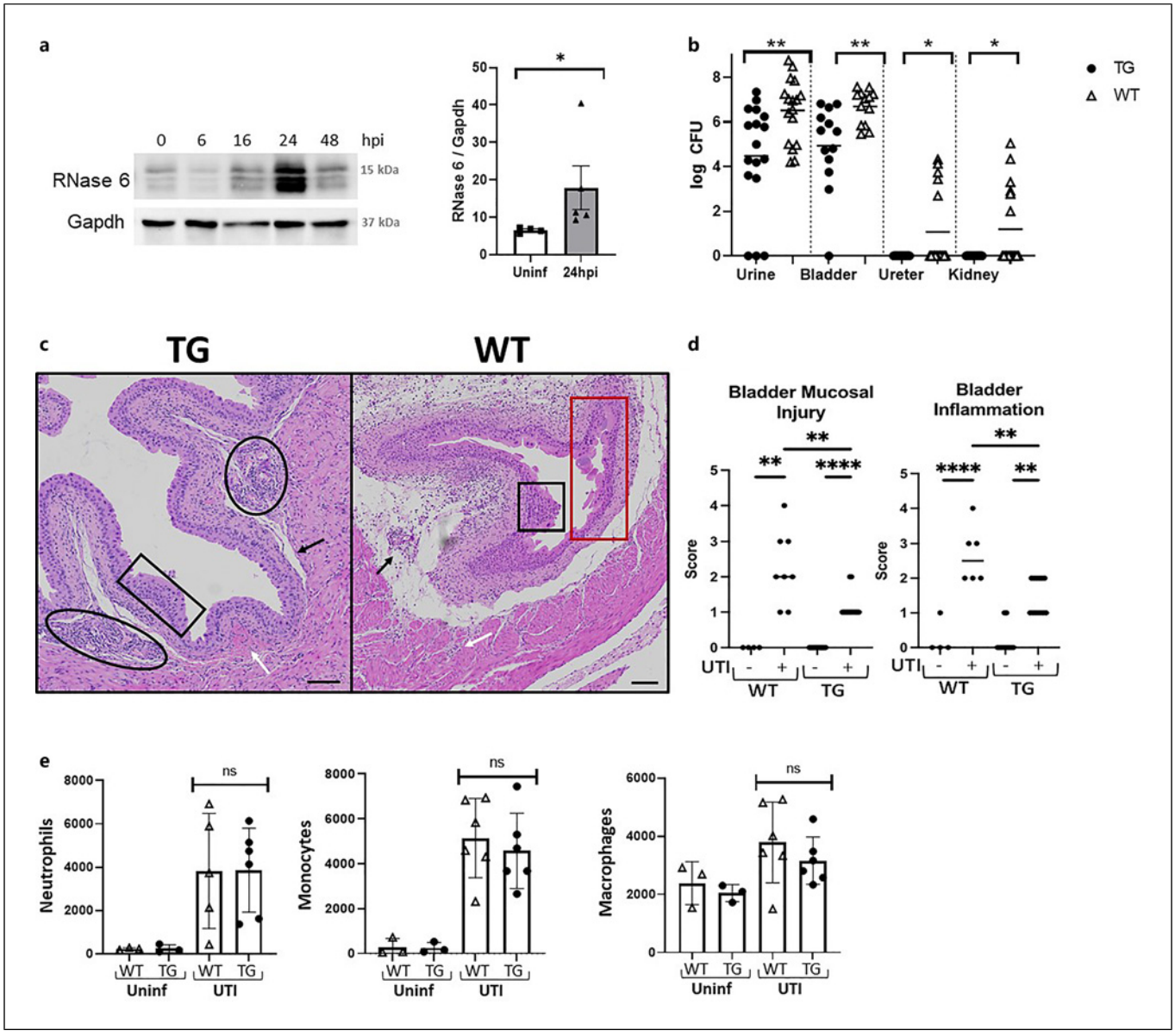

Fig. 2. *RNASE6* transgene exerts a protective role during experimental cystitis. **a** Representative Western blot shows increased RNase 6 protein expression in *RNASE6* transgenic bladder extracts at indicated times after transurethral UPEC inoculation. Gapdh is included as a loading control. The graph depicts increased bladder RNase 6/Gapdh levels 24 hpi compared to uninfected bladders by densitometry. (Bars indicate mean ± SEM for each condition; n = 4 bladders/group; $p = 0.0159$, Mann-Whitney U test.) **b** Reduced UPEC burden in *RNASE6* transgenic mice (TG) 24 hpi compared to non-transgenic, wild-type (WT) controls (**$p < 0.01$; *$p < 0.05$; Mann-Whitney U Test; n = 13–17 mice/group). Horizontal lines indicate the geometric mean for each condition. **c** *RNASE6* transgenic bladders (TG) manifest minimal to mild edema (black arrow), multifocal, submucosal suppurative inflammation (black circles), and focal hemorrhage (white arrow). Throughout the mucosa, there is multifocal hyperplasia (black box), with degenerate urothelial cells and neutrophilic inflammation. Conversely, non-transgenic bladders (WT) show severe submucosal edema and suppurative inflammation (black arrow) with foci of hemorrhage 24 hpi. The mucosa is variably hyperplastic (black box) or superficially eroded with sloughing of superficial urothelial cells (red box). Inflammation extends into the muscularis (white arrow). Scale bars indicate 100 μm. **d** Bladder inflammation and mucosal injury scores in *RNASE6* transgenic mice and controls (**$p < 0.01$; ****$p < 0.0001$; Mann-Whitney U Test; n = 4–13 mice/group; horizontal bars indicate median values for each group). **e** Flow cytometry identifies comparable numbers of neutrophils ($CD45^+/CD11B^+/Ly6C^-/Ly6G^+$), monocytes ($CD45^+/CD11B^+/Ly6G^-/Ly6C^+$), and macrophages ($Ly6C^-/Ly6G^-/MHC\text{-}II^+/F4/80^+$) in *RNASE6* transgenic bladders and non-transgenic controls at baseline and 24 hpi (ns: not significant, Mann-Whitney U test; bars indicate mean ± SD for each group). hpi, hours postinfection.

ureters, and kidneys of infected *RNASE6* transgenic mice compared to non-transgenic controls (Fig. 2b). However, we did not observe changes in UPEC intracellular bacterial community counts in transgenic and control bladders 6 hpi (online suppl. Fig. S2C). Transgenic mice exhibited reduced mucosal injury and bladder inflammation scores 24 hpi (Fig. 2c, d) but did not differ from non-transgenic controls with regard to phagocyte recruitment (Fig. 2e). Subsequently, we did not note any difference in UPEC burden between *RNASE6* transgenic and non-transgenic controls 48 and 72 hpi (online suppl. Fig. S2D, E). Thus, human RNase 6 provides a temporally delimited window of protection to promote bacterial clearance and reduce tissue injury during experimental UPEC-induced cystitis.

Monocytes and Macrophages Are the Main Cellular Sources of RNase 6 during Cystitis. Based on our previous studies and the published literature, we hypothesized that phagocytes such as neutrophils, monocytes, and macrophages were the likeliest sources of RNase 6 [11, 30, 31]. Using immunofluorescence microscopy, we detected RNase 6 in a granular distribution within cells in the submucosa of uninfected bladders (Fig. 3a). Following UPEC infection, RNase 6+ cells increased in abundance and infiltrated the urothelium and submucosa (Fig. 3b, c). In rare instances, RNase 6+ cells were observed in the vicinity of UPEC intracellular bacterial communities. RNase 6+ cells did not express the neutrophil-specific antigen, Ly6G (Fig. 3d, g). To investigate whether monocytes and macrophages are cellular sources of RNase 6, we generated *RNASE6* transgenic; *Cx3cr1*$^{GFP/+}$; *Ccr2*$^{RFP/+}$ reporter mice, in which Cx3cr1+ macrophages express the green fluorescent protein (GFP); Ccr2+ monocytes express the red fluorescent protein (RFP); and monocyte-derived macrophages express both GFP and RFP [32, 33]. RNase 6 localized to distinct Cx3Cr1^{GFP+} macrophages and Ccr2^{RFP+} monocytes in uninfected bladders (Fig. 3e, h). Following UPEC infection, RNase 6 localized primarily to Ccr2^{RFP+}; Cx3Cr1^{GFP+} monocyte-derived macrophages (Fig. 3f, i). These finding confirm that monocytes and macrophages are a critical cellular source of RNase 6 during UTI.

Human RNase 6 Promotes UPEC Killing by Macrophages. Since macrophages exert potent antimicrobial activity and are a prominent source of RNase 6 during experimental cystitis, we investigated the contributions of RNase 6 to UPEC killing by BMDM in vitro. *RNASE6* transgenic BMDM expressed human RNase 6 protein at baseline (Fig. 4a), and UPEC exposure did not lead to substantial changes in RNase 6 protein levels in the cellular fraction or supernatants (online suppl. Fig. S3A). We challenged *RNASE6* transgenic and control BMDM with UPEC at varying MOI, and quantified extracellular, attached, and intracellular CFU (Fig. 4b). While we did not observe differences in extracellular or attached UPEC between genotypes (online suppl. Fig. S3b), we recovered significantly fewer intracellular CFU from *RNASE6* transgenic BMDMs compared to controls (Fig. 4c). *RNASE6* transgenic and non-transgenic BMDM exhibited similar levels of apoptosis and necrosis as well as cytokine elicitation following UPEC exposure and did not differ in their phagocytic capacities (Fig. 4d, f). These studies argued against a difference between *RNASE6* transgenic and control BMDM in their overall state of activation. Altogether these findings support a role for macrophage-derived RNase 6 in intracellular killing of phagocytosed UPEC.

Discussion

While mammalian genomes encode hundreds of proteins and peptides with established antimicrobial activity in vitro, their functional significance remains largely untested in vivo. In a similar vein, we previously identified RNase 6 as a leukocyte-derived AMP with bactericidal activity in vitro, with a preference toward Gram-negative species and in particular toward UPEC [11], but the physiological roles of RNase 6 during UTI remained uncertain. Accordingly, the purposes of this study were: to test the hypothesis that RNase 6 promotes antimicrobial activity toward UPEC in vivo; to define the cellular sources of RNase 6 at steady-state and following UTI; and to test the antimicrobial activity of RNase 6 toward UPEC at a cellular level within a macrophage context.

In this study, we demonstrated that human RNase 6 can be safely and effectively over-expressed in mice. We found that the expression of RNase 6 protein was tightly regulated during cystitis, and its upregulation 24 hpi was associated with limited UPEC burden and tissue injury at this time point in *RNASE6* transgenic mice. Use of the *Cx3cr1*^{GFP} and *Ccr2*^{RFP} reporter alleles identified monocytes and macrophages as the main cellular sources of human RNase 6 during experimental UTI. Experiments in BMDM from *RNASE6* transgenic and non-transgenic mice further established that RNase 6 promotes the killing of phagocytosed UPEC. Our findings indicate that human RNase 6 expression in macrophages is an antimicrobial mechanism that limits UPEC colonization within the urinary tract.

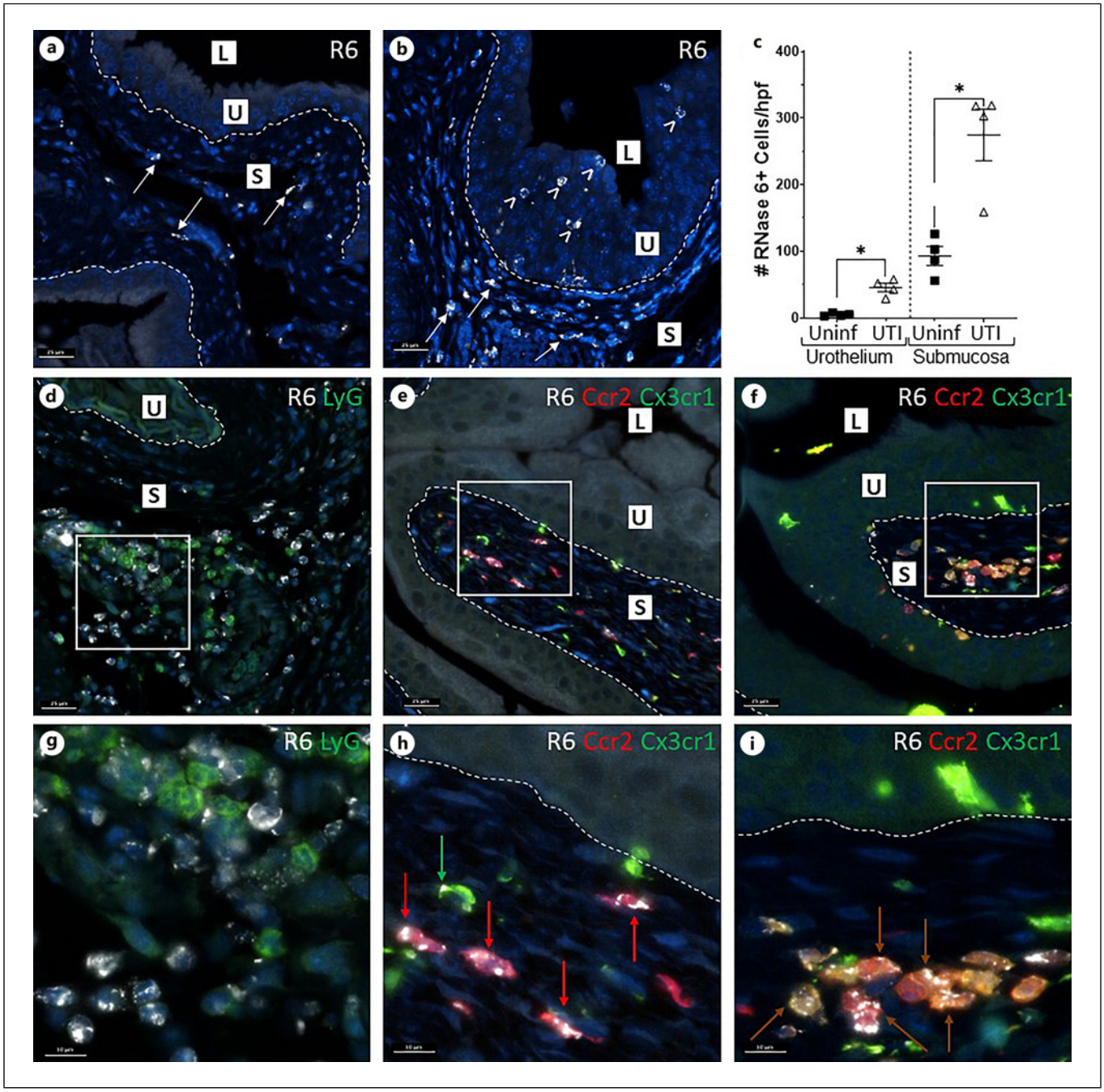

Fig. 3. Cellular sources of RNase 6 within the bladder at baseline and following UPEC infection. **a** Immunofluorescence microscopy identifies RNase6 reactivity (white arrows) in within non-infected bladder submucosal cells. Dashed lines indicate the urothelial basement membrane. **b** Following UPEC infection, RNase 6 cells continue to localize to submucosa (white arrows) and infiltrate the urothelium (white arrowheads). **c** The graph depicts the number and distribution of RNase 6+ cells per high power field (hpf) in uninfected versus 24 h infected bladders (n = 4 bladders/group; *p = 0.0286, Mann-Whitney U test; horizontal bars indicate mean ± SEM for each condition). **d**, **g** 24 h after UPEC infection, RNase 6+ cells do not express the neutrophil specific antigen, Ly6G. **e**, **h** RNase 6+ cells (white) co-express Ccr2 (red arrows) or Cx3cr1 (green arrow) in the absence of UTI. Ccr2+ and Cx3cr1+ cells were identified using antibodies raised against RFP and GFP, respectively, in *RNASE6*+; *Ccr2*$^{RFP/+}$; *Cx3cr1*$^{GFP/+}$ mice. **f**, **i** 24 h after UPEC infection, RNase 6 localizes primarily to Ccr2+; Cx3cr1+ monocyte-derived macrophages (brown arrows). Representative micrographs from 4 to 6 separate bladders are shown. Scale bars represent 25 microns (**a**–**f**) and 10 microns (**g**–**i**). L, Lumen; U, Urothelium; S, Submucosa.

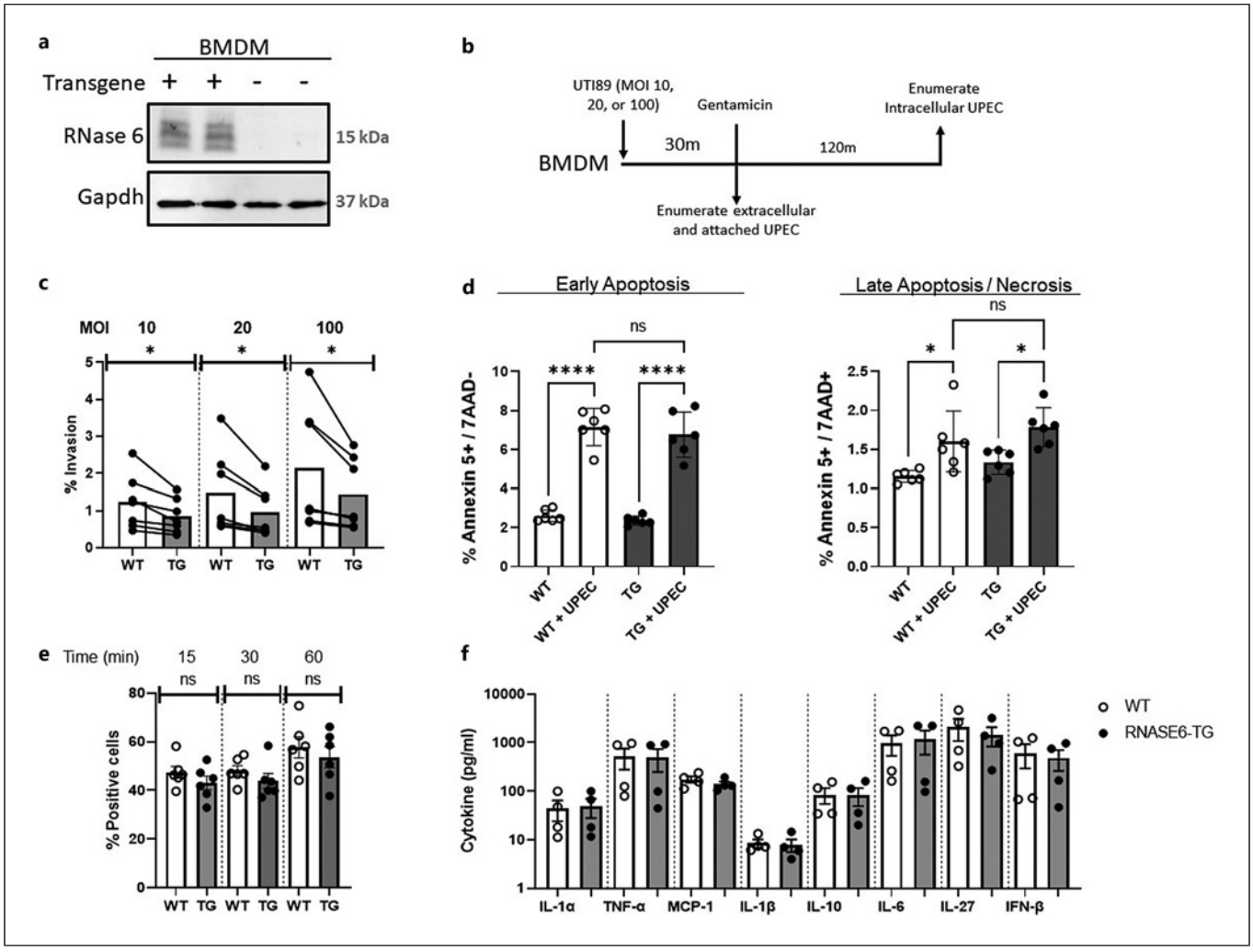

Fig. 4. Macrophage-derived RNase 6 promotes elimination of intracellular UPEC in vitro. **a** Expression of RNase 6 protein by *RNASE6* transgenic in bone marrow-derived macrophages (BMDM). **b** Experimental design to test the contributions of RNase 6 to UPEC killing by BMDM. Time in minutes (m) is indicated. **c** Reduced recovery of intracellular UPEC from *RNASE6* transgenic BMDM (TG) compared to non-transgenic controls (WT), at the indicated MOI. Results from 6 experiments are shown. Each data point represents the average of 6 technical replicates from a single experiment. The bar designates the mean across experiments. Paired data are connected by lines and analyzed by paired *t* test (*$p < 0.05$). **d** WT and *RNASE6* transgenic BMDM exhibit comparable levels of apoptosis and necrosis at baseline and following UPEC exposure (MOI 10) for 30 min (early apoptosis) and 3 h (late apoptosis/necrosis)(*$p < 0.0001$, ANOVA). **e** WT and *RNASE6* transgenic BMDM do not differ in their phagocytic capacity of fluorescein-labeled *E. coli* K-12 bioparticles. **f** Similar magnitudes of cytokine elicitation by UPEC (MOI 10) in *RNASE6* transgenic and WT BMDM 24 hpi.

Previous studies have relied upon depletion of monocytes and macrophages to implicate these cells in the innate immune response to UTI, but the mechanisms responsible for UPEC clearance have been unclear [16, 17]. Some have argued that monocytes and macrophages serve an indirect role in promoting neutrophil recruitment and activation through the production of cytokines and chemokines [15, 17, 34]. Others have claimed that macrophages directly exert antimicrobial activity during cystitis by migrating from the submucosa to the urothelium, where they phagocytose UPEC [35]. Even so, the precise antibacterial mechanisms employed by macrophages during UTI remain incompletely understood. Some of the primary antimicrobial mechanisms triggered by UPEC in macrophages include: the

activation of the inflammasome and caspase-1-dependent processing of pro-IL-1β [36]; macrophage-mediated zinc poisoning [37]; and the suppression of iron retention and lipocalin 2 production [38]. In this context, we have identified human RNase 6 as an additional, novel effector mechanism employed by macrophages to directly target invading uropathogens such as UPEC.

In this regard, there are features of RNase 6 that make it ideally poised to serve as an instrumental antimicrobial effector toward UPEC in macrophages. To begin with, RNase 6 has been identified as a lysosomal resident protein [39]. This compartmentalization may allow RNase 6 to reach high concentrations, as has been recently shown for RNase 2 and RNase T2 [40], while not causing cytotoxicity. Furthermore, UPEC has been shown to reside within Lamp1+ vesicles following its phagocytosis by macrophages – a scenario that favors its encounter with RNase 6 [29]. As a cationic protein, RNase 6 binds to bacterial lipopolysaccharide with high affinity, permitting its association with the Gram-negative wall of UPEC [41]. Through its amino (N-) terminus, RNase 6 promotes the agglutination of UPEC, thereby producing densely packed bacterial aggregates [41]. Finally, hydrophobic residues within the N-terminus of RNase 6 allow it to disrupt lipid bilayers and bacterial membranes, dissipating electrochemical gradients and resulting in potent bactericidal activity [41]. These attributes of RNase 6 make this AMP a compelling candidate for therapeutic strategies that seek to increase its levels, activity, or both, in order to prevent and treat UTI.

Work from our group has previously established key roles for epithelial-derived RNase 4 and RNase 7 in host defense against UTI [13, 27, 28, 42, 43]. However, the contributions of leukocyte-derived RNases during UTI in vivo have remained unknown. In this study, we have begun to fill this knowledge gap by implicating RNase 6 as an intracellular AMP that promotes UPEC killing following bacterial phagocytosis by macrophages in vitro and in the context of experimental UTI in vivo. While RNase 6 offered a window of protection by reducing bacterial burden and tissue injury during acute cystitis, further studies are warranted to understand whether RNase 6 can limit chronic and recurrent UTI. In addition, future, complementary experiments in *Rnase6* deficient mice are needed to fully comprehend the contributions of RNase 6 to macrophage antimicrobial activity and UTI susceptibility in vivo.

Acknowledgments

We thank Dr. Dale Cowley (Transviragen, Inc.) for generating *RNASE6* transgenic mice. Figure 1 was created in part with BioRender.com.

Statement of Ethics

This study protocol was reviewed and approved by the Institutional Animal Care and Use Committee at the Abigail Wexner Research Institute at Nationwide Children's Hospital (Protocol Number AR13-00057).

Conflict of Interest Statement

The authors have no conflicts of interest to disclose.

Funding Sources

This work was supported by the National Institutes of Health (NIDDK) R01 DK115737 and R01DK114035 (JDS), R03 DK118306 (BB), K01 DK128379-01 (JRR). We thank the *Agencia Estatal de Investigación* for the financial support to EB (PID2019-106123GB-I00/AEI/10.13039/501100011033). The Ohio State University Comparative Pathology and Mouse Phenotyping Shared Resource is supported by the National Institutes of Health (NCI) P30 CA016058. This project was supported by the Clinical and Translational Intramural Funding Program through the Abigail Wexner Research Institute at Nationwide Children's Hospital (Columbus, OH, USA).

Author Contributions

Juan de Dios Ruiz-Rosado and Hanna Cortado: designed and performed main experiments involving transgenic mice, analyzed data, and manuscript preparation. Macie Kerscmar: immunofluorescence microscopy. Birong Li: performed experimental cystitis and analyzed UPEC burden data. Gregory Ballash: evaluation of bladder histopathology. Israel Cotzomi-Ortega and Yuriko I. Sanchez-Zamora: investigation of BMDM phagocytosis and viability. Christina Ching and Sudipti Gupta: enumeration of IBC during experimental cystitis. Ester Boix: data analysis and manuscript preparation. Ashley R. Jackson: immunofluorescence microscopy. John David Spencer: experimental design and manuscript preparation. Brian Becknell: experimental design, data analysis, and manuscript preparation.

Data Availability Statement

All data generated or analyzed during this study are included in this article. Further inquiries can be directed to the corresponding author.

References

1 Tullus K, Shaikh N. Urinary tract infections in children. Lancet. 2020;395(10237):1659–68.
2 Mishra OP, Abhinay A, Prasad R. Urinary infections in children. Indian J Pediatr. 2013;80(10):838–43.
3 Spencer JD, Schwaderer A, McHugh K, Hains DS. Pediatric urinary tract infections: an analysis of hospitalizations, charges, and costs in the USA. Pediatr Nephrol. 2010;25(12):2469–75.
4 Freedman AL, Urologic Diseases in America Project. Urologic diseases in North America Project: trends in resource utilization for urinary tract infections in children. J Urol. 2005;173(3):949–54.
5 Edlin RS, Shapiro DJ, Hersh AL, Copp HL. Antibiotic resistance patterns of outpatient pediatric urinary tract infections. J Urol. 2013;190(1):222–7.
6 Ching C, Schwartz L, Spencer JD, Becknell B. Innate immunity and urinary tract infection. Pediatr Nephrol. 2020;35(7):1183–92.
7 Becknell B, Schwaderer A, Hains DS, Spencer JD. Amplifying renal immunity: the role of antimicrobial peptides in pyelonephritis. Nat Rev Nephrol. 2015;11(11):642–55.
8 Ali AS, Townes CL, Hall J, Pickard RS. Maintaining a sterile urinary tract: the role of antimicrobial peptides. J Urol. 2009;182(1):21–8.
9 Lazzaro BP, Zasloff M, Rolff J. Antimicrobial peptides: application informed by evolution. Science. 2020;368(6490):eaau5480.
10 Becknell B, Ching C, Spencer JD. The responses of the ribonuclease A superfamily to urinary tract infection. Front Immunol. 2019;10:2786.
11 Becknell B, Eichler TE, Beceiro S, Li B, Easterling RS, Carpenter AR, et al. Ribonucleases 6 and 7 have antimicrobial function in the human and murine urinary tract. Kidney Int. 2015;87(1):151–61.
12 Chromek M, Slamová Z, Bergman P, Kovács L, Podracká L, Ehrén I, et al. The antimicrobial peptide cathelicidin protects the urinary tract against invasive bacterial infection. Nat Med. 2006;12(6):636–41.
13 Spencer JD, Schwaderer AL, Wang H, Bartz J, Kline J, Eichler T, et al. Ribonuclease 7, an antimicrobial peptide upregulated during infection, contributes to microbial defense of the human urinary tract. Kidney Int. 2013;83(4):615–25.
14 Schwartz L, de Dios Ruiz-Rosado J, Stonebrook E, Becknell B, Spencer JD. Uropathogen and host responses in pyelonephritis. Nat Rev Nephrol. 2023;19(10):658–71.
15 Berry MR, Mathews RJ, Ferdinand JR, Jing C, Loudon KW, Wlodek E, et al. Renal sodium gradient orchestrates a dynamic antibacterial defense zone. Cell. 2017;170(5):860–74 e19.
16 Carey AJ, Sullivan MJ, Duell BL, Crossman DK, Chattopadhyay D, Brooks AJ, et al. Uropathogenic Escherichia coli engages CD14-dependent signaling to enable bladder-macrophage-dependent control of acute urinary tract infection. J Infect Dis. 2016;213(4):659–68.
17 Schiwon M, Weisheit C, Franken L, Gutweiler S, Dixit A, Meyer-Schwesinger C, et al. Crosstalk between sentinel and helper macrophages permits neutrophil migration into infected uroepithelium. Cell. 2014;156(3):456–68.
18 Hannan TJ, Roberts PL, Riehl TE, van der Post S, Binkley JM, Schwartz DJ, et al. Inhibition of cyclooxygenase-2 prevents chronic and recurrent cystitis. EBioMedicine. 2014;1(1):46–57.
19 Ruiz-Rosado JD, Robledo-Avila F, Cortado H, Rangel-Moreno J, Justice SS, Yang C, et al. Neutrophil-macrophage imbalance drives the development of renal scarring during experimental pyelonephritis. J Am Soc Nephrol. 2021;32(1):69–85.
20 Lacerda Mariano L, Rousseau M, Varet H, Legendre R, Gentek R, Saenz Coronilla J, et al. Functionally distinct resident macrophage subsets differentially shape responses to infection in the bladder. Sci Adv. 2020;6(48):eabc5739.
21 Mulvey MA, Schilling JD, Hultgren SJ. Establishment of a persistent Escherichia coli reservoir during the acute phase of a bladder infection. Infect Immun. 2001;69(7):4572–9.
22 Hung CS, Dodson KW, Hultgren SJ. A murine model of urinary tract infection. Nat Protoc. 2009;4(8):1230–43.
23 Hopkins W, Gendron-Fitzpatrick A, McCarthy DO, Haine JE, Uehling DT. Lipopolysaccharide-responder and nonresponder C3H mouse strains are equally susceptible to an induced Escherichia coli urinary tract infection. Infect Immun. 1996;64(4):1369–72.
24 Li B, Haridas B, Jackson AR, Cortado H, Mayne N, Kohnken R, et al. Inflammation drives renal scarring in experimental pyelonephritis. Am J Physiol Renal Physiol. 2017;312(1):F43–53.
25 Ching CB, Gupta S, Li B, Cortado H, Mayne N, Jackson AR, et al. Interleukin-6/Stat3 signaling has an essential role in the host antimicrobial response to urinary tract infection. Kidney Int. 2018;93(6):1320–9.
26 Schwartz DJ, Chen SL, Hultgren SJ, Seed PC. Population dynamics and niche distribution of uropathogenic Escherichia coli during acute and chronic urinary tract infection. Infect Immun. 2011;79(10):4250–9.
27 Spencer JD, Schwaderer AL, Dirosario JD, McHugh KM, McGillivary G, Justice SS, et al. Ribonuclease 7 is a potent antimicrobial peptide within the human urinary tract. Kidney Int. 2011;80(2):174–80.
28 Eichler T, Bender K, Murtha MJ, Schwartz L, Metheny J, Solden L, et al. Ribonuclease 7 shields the kidney and bladder from invasive uropathogenic Escherichia coli infection. J Am Soc Nephrol. 2019;30(8):1385–97.
29 Bokil NJ, Totsika M, Carey AJ, Stacey KJ, Hancock V, Saunders BM, et al. Intramacrophage survival of uropathogenic Escherichia coli: differences between diverse clinical isolates and between mouse and human macrophages. Immunobiology. 2011;216(11):1164–71.
30 Rosenberg HF, Dyer KD. Molecular cloning and characterization of a novel human ribonuclease (RNase k6): increasing diversity in the enlarging ribonuclease gene family. Nucleic Acids Res. 1996;24(18):3507–13.
31 Lu L, Arranz-Trullén J, Prats-Ejarque G, Pulido D, Bhakta S, Boix E. Human antimicrobial RNases inhibit intracellular bacterial growth and induce autophagy in mycobacteria-infected macrophages. Front Immunol. 2019;10:1500.
32 Saederup N, Cardona AE, Croft K, Mizutani M, Cotleur AC, Tsou CL, et al. Selective chemokine receptor usage by central nervous system myeloid cells in CCR2-red fluorescent protein knock-in mice. PLoS One. 2010;5(10):e13693.
33 Jung S, Aliberti J, Graemmel P, Sunshine MJ, Kreutzberg GW, Sher A, et al. Analysis of fractalkine receptor CX(3)CR1 function by targeted deletion and green fluorescent protein reporter gene insertion. Mol Cell Biol. 2000;20(11):4106–14.
34 Stewart BJ, Ferdinand JR, Young MD, Mitchell TJ, Loudon KW, Riding AM, et al. Spatiotemporal immune zonation of the human kidney. Science. 2019;365(6460):1461–6.
35 Bottek J, Soun C, Lill JK, Dixit A, Thiebes S, Beerlage AL, et al. Spatial proteomics revealed a CX3CL1-dependent crosstalk between the urothelium and relocated macrophages through IL-6 during an acute bacterial infection in the urinary bladder. Mucosal Immunol. 2020;13(4):702–14.
36 Murthy AMV, Sullivan MJ, Nhu NTK, Lo AW, Phan MD, Peters KM, et al. Variation in hemolysin A expression between uropathogenic Escherichia coli isolates determines NLRP3-dependent vs. -independent macrophage cell death and host colonization. FASEB J. 2019;33(6):7437–50.
37 Stocks CJ, Phan MD, Achard MES, Nhu NTK, Condon ND, Gawthorne JA, et al. Uropathogenic Escherichia coli employs both evasion and resistance to subvert innate immune-mediated zinc toxicity for dissemination. Proc Natl Acad Sci U S A. 2019;116(13):6341–50.
38 Owusu-Boaitey N, Bauckman KA, Zhang T, Mysorekar IU. Macrophagic control of the response to uropathogenic E. coli infection by regulation of iron retention in an IL-6-dependent manner. Immun Inflamm Dis. 2016;4(4):413–26.

39 Sleat DE, Sun P, Wiseman JA, Huang L, El-Banna M, Zheng H, et al. Extending the mannose 6-phosphate glycoproteome by high resolution/accuracy mass spectrometry analysis of control and acid phosphatase 5-deficient mice. Mol Cell Proteomics. 2013;12(7):1806–17.
40 Ostendorf T, Zillinger T, Andryka K, Schlee-Guimaraes TM, Schmitz S, Marx S, et al. Immune sensing of synthetic, bacterial, and Protozoan RNA by toll-like receptor 8 requires coordinated processing by RNase T2 and RNase 2. Immunity. 2020;52(4):591–605 e6.
41 Pulido D, Arranz-Trullén J, Prats-Ejarque G, Velázquez D, Torrent M, Moussaoui M, et al. Insights into the antimicrobial mechanism of action of human RNase6: structural determinants for bacterial cell agglutination and membrane permeation. Int J Mol Sci. 2016;17(4):552.
42 Bender K, Schwartz LL, Cohen A, Vasquez CM, Murtha MJ, Eichler T, et al. Expression and function of human ribonuclease 4 in the kidney and urinary tract. Am J Physiol Renal Physiol. 2021;320(5):F972–83.
43 Pierce KR, Eichler T, Mosquera Vasquez C, Schwaderer AL, Simoni A, Creacy S, et al. Ribonuclease 7 polymorphism rs1263872 reduces antimicrobial activity and associates with pediatric urinary tract infections. J Clin Invest. 2021;131(22):e149807.